Draft version February 26, 2023
Typeset using LaTeX default style in AASTeX631

Full velocities and propagation directions of coronal mass ejections inferred from simultaneous full-disk imaging and Sun-as-a-star spectroscopic observations

Hong-peng Lu,[1] Hui Tian,[1,2,3,*] He-chao Chen,[4,1] Yu Xu,[1,5] Zhen-yong Hou,[1] Xian-yong Bai,[3] Guang-yu Tan,[1] Zi-hao Yang,[1] and Jie Ren[1]

[1] *School of Earth and Space Sciences, Peking University, Beijing, 100871, People's Republic of China*
[2] *Key Laboratory of Solar Activity and Space Weather, National Space Science Center, Chinese Academy of Sciences, Beijing 100190, People's Republic of China*
[3] *National Astronomical Observatories, Chinese Academy of Sciences, Beijing 100101, People's Republic of China*
[4] *School of Physics and Astronomy, Yunnan University, Kunming 650500, People's Republic of China*
[5] *Leibniz Institute for Astrophysics Potsdam, An der Sternwarte 16, D-14482 Potsdam, Germany*

ABSTRACT

Coronal mass ejections (CMEs) are violent ejections of magnetized plasma from the Sun, which can trigger geomagnetic storms, endanger satellite operations and destroy electrical infrastructures on the Earth. After systematically searching Sun-as-a-star spectra observed by the Extreme-ultraviolet Variability Experiment (EVE) onboard the *Solar Dynamics Observatory* (SDO) from May 2010 to May 2022, we identified eight CMEs associated with flares and filament eruptions by analyzing the blue-wing asymmetry of the O III 52.58 nm line profiles. Combined with images simultaneously taken by the 30.4 nm channel of the Atmospheric Imaging Assembly onboard SDO, the full velocity and propagation direction for each of the eight CMEs are derived. We find a strong correlation between geomagnetic indices (Kp and Dst) and the angle between the CME propagation direction and the Sun-Earth line, suggesting that Sun-as-a-star spectroscopic observations at EUV wavelengths can potentially help to improve the prediction accuracy of the geoeffectiveness of CMEs. Moreover, an analysis of synthesized long-exposure Sun-as-a-star spectra implies that it is possible to detect CMEs from other stars through blue-wing asymmetries or blueshifts of spectral lines.

Keywords: Solar coronal mass ejections (310) — Stellar coronal mass ejections (1881) — Solar filament eruptions (1981) — Spectroscopy (1558) — Space weather (2037)

SUPPLEMENTARY

* huitian@pku.edu.cn

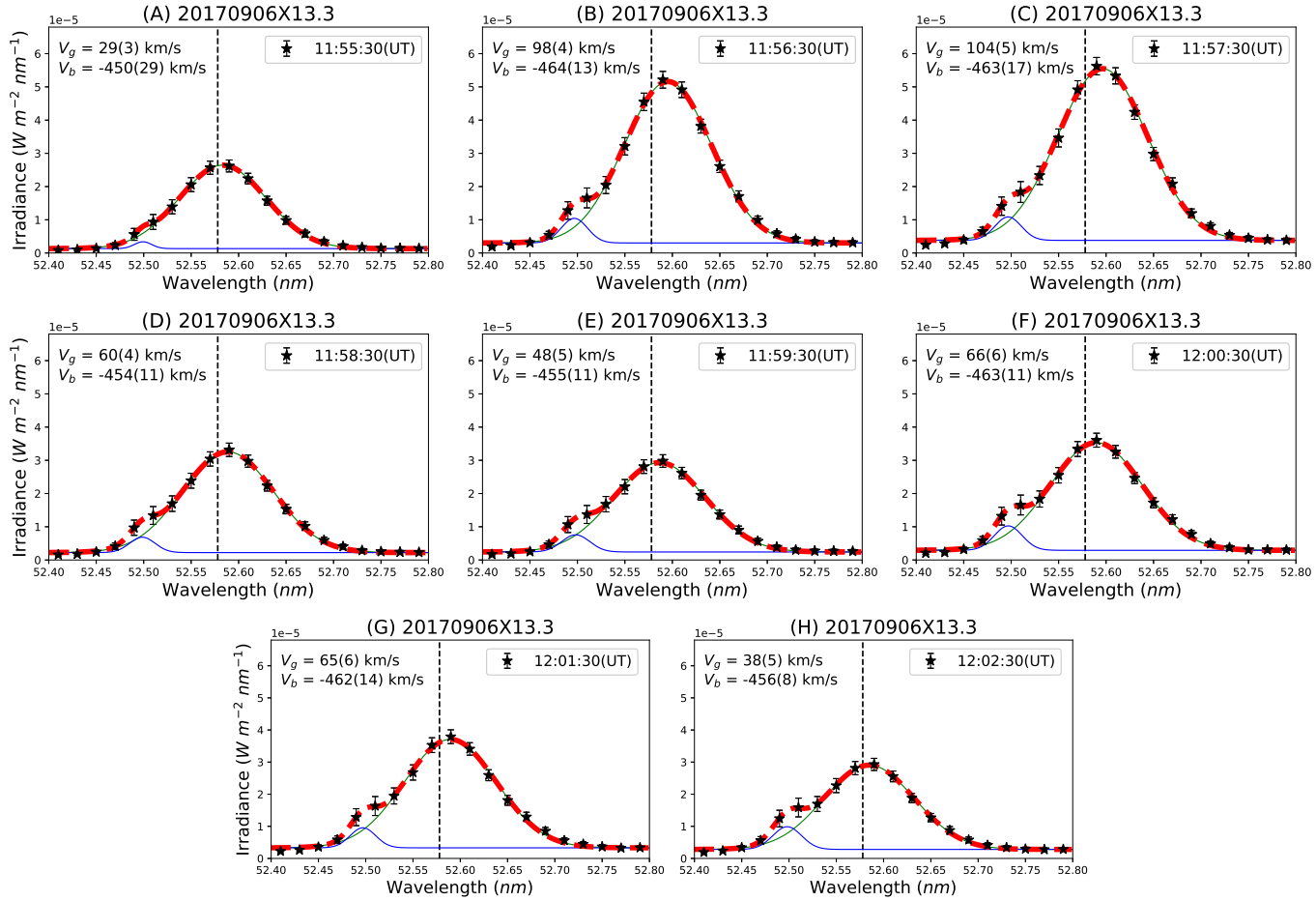

Figure 1. Double Gaussian fitting results for eight O III 52.58 nm line profiles taken during CME 2 (20170906X13.3). The eight panels are similar to those in Figure 3 of the paper.

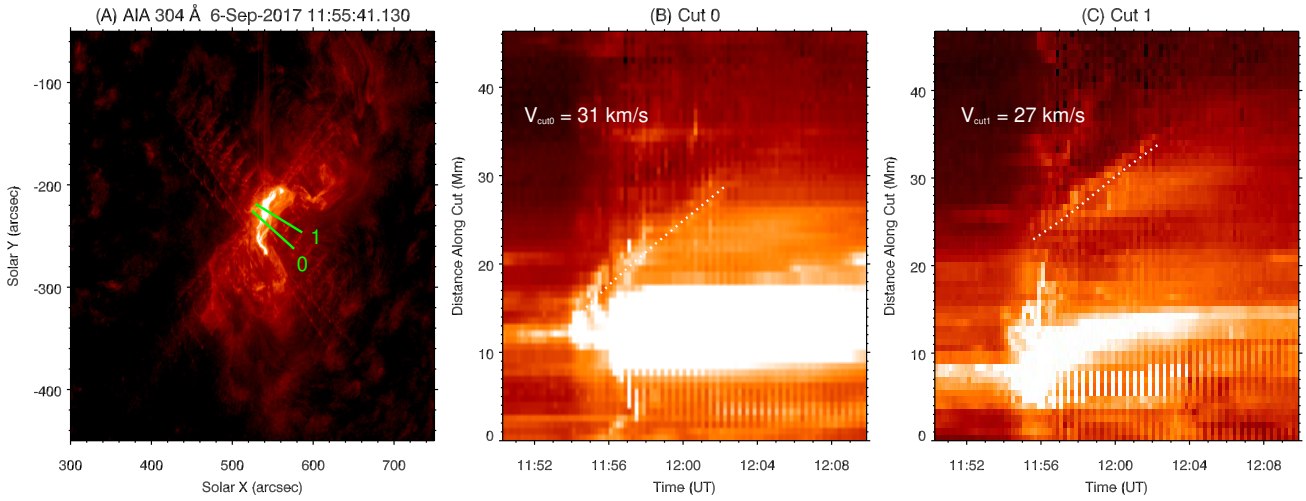

Figure 2. Ejecta associated with CME 2 (20170906X13.3) in SDO/AIA 30.4 nm images. The three panels are similar to those in Figure 4 of the paper.
(An animation of this figure is available.)

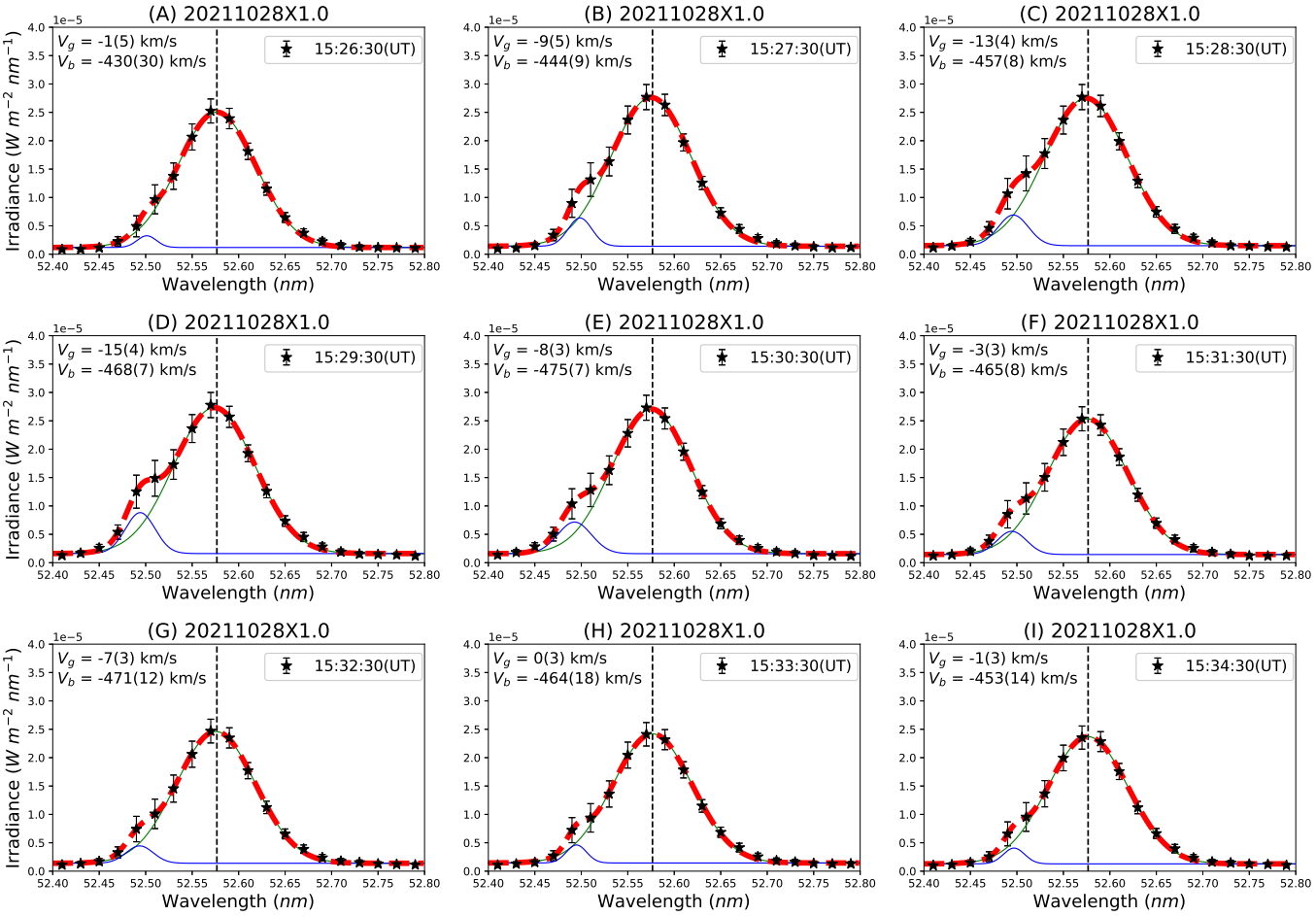

Figure 3. Double Gaussian fitting results for nine O III 52.58 nm line profiles taken during CME 3 (20211028X1.0). The nine panels are similar to those in Figure 3 of the paper.

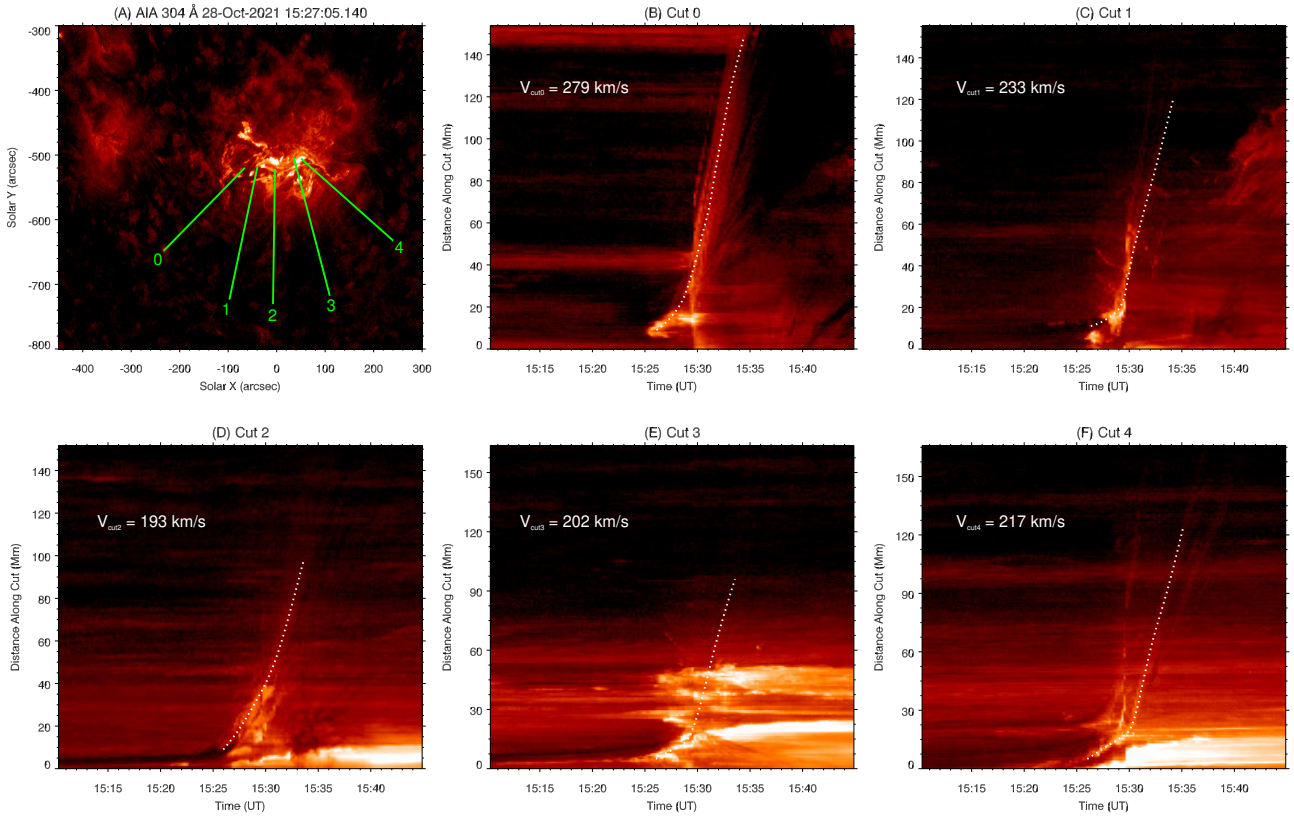

Figure 4. Ejecta associated with CME 3 (20211028X1.0) in SDO/AIA 30.4 nm images. The six panels are similar to those in Figure 4 of the paper.
(An animation of this figure is available.)

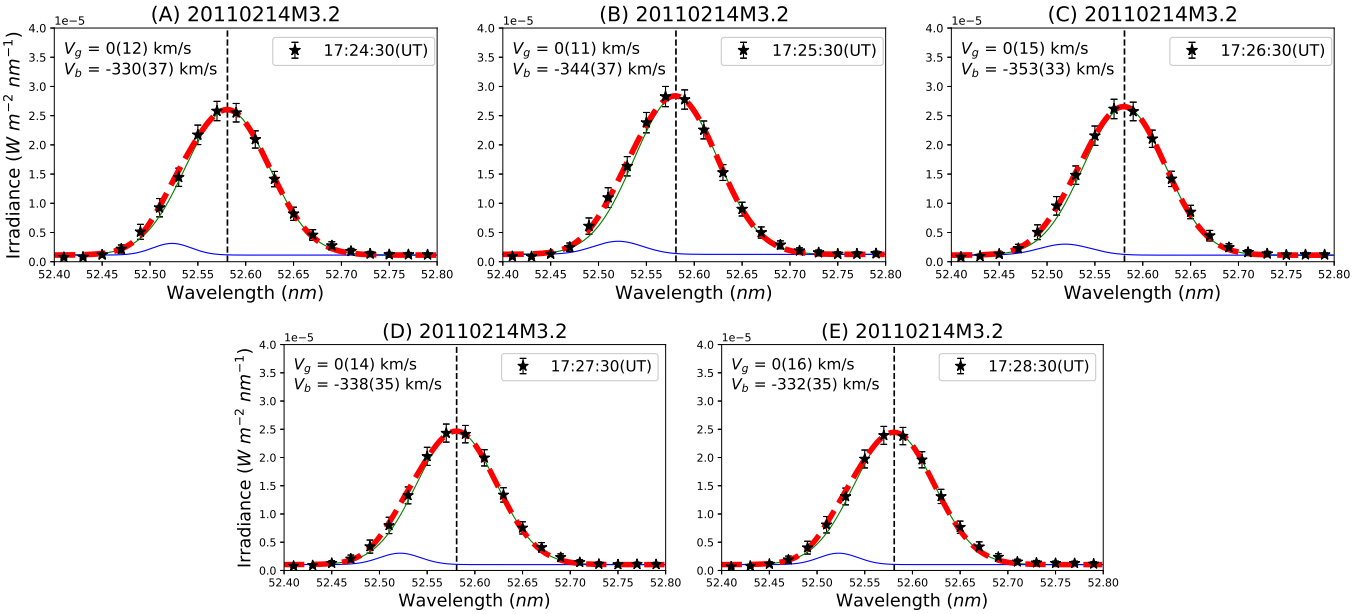

Figure 5. Double Gaussian fitting results for five O III 52.58 nm line profiles taken during CME 4 (20110214M3.2). The five panels are similar to those in Figure 3 of the paper.

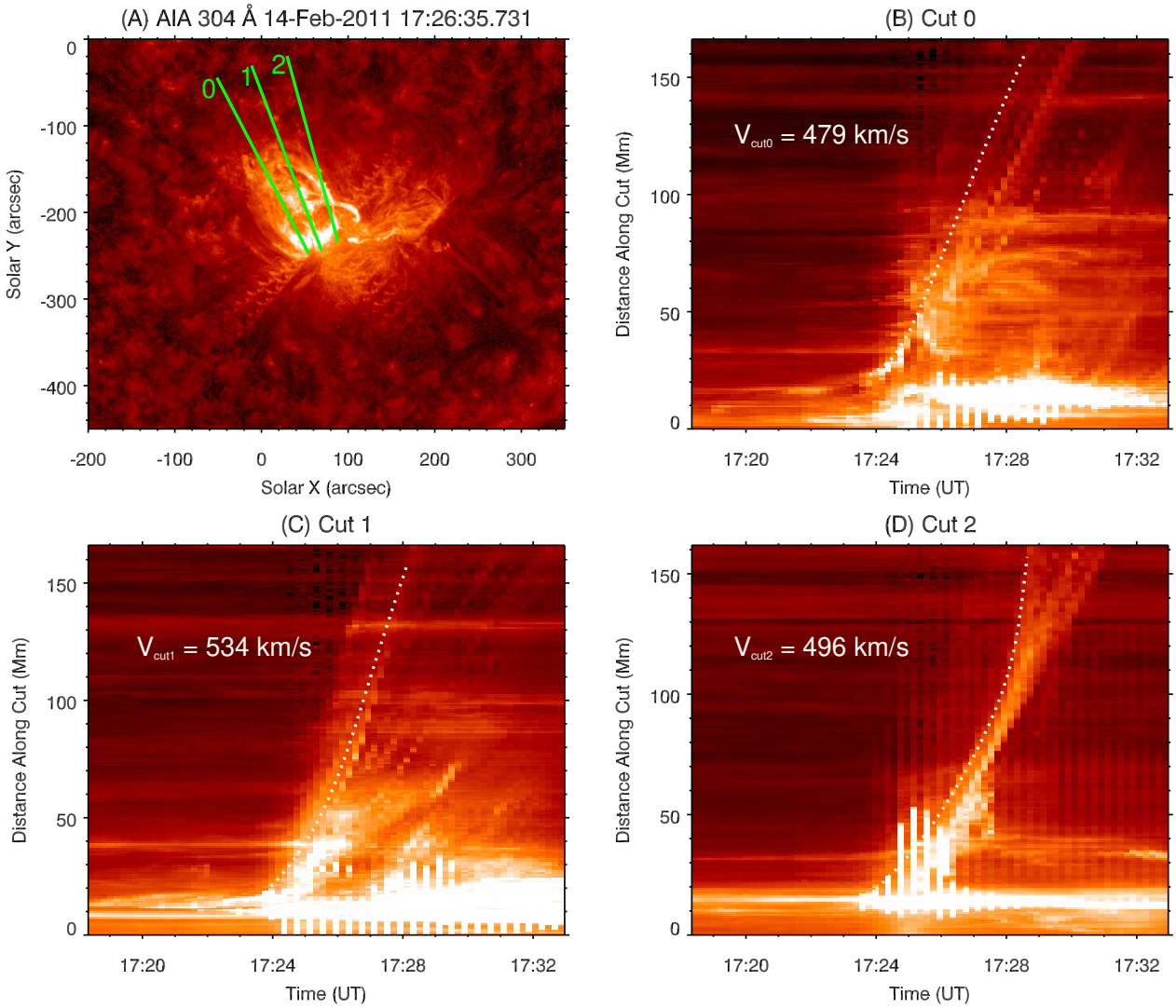

Figure 6. Ejecta associated with CME 4 (20110214M3.2) in SDO/AIA 30.4 nm images. The four panels are similar to those in Figure 4 of the paper.
(An animation of this figure is available.)

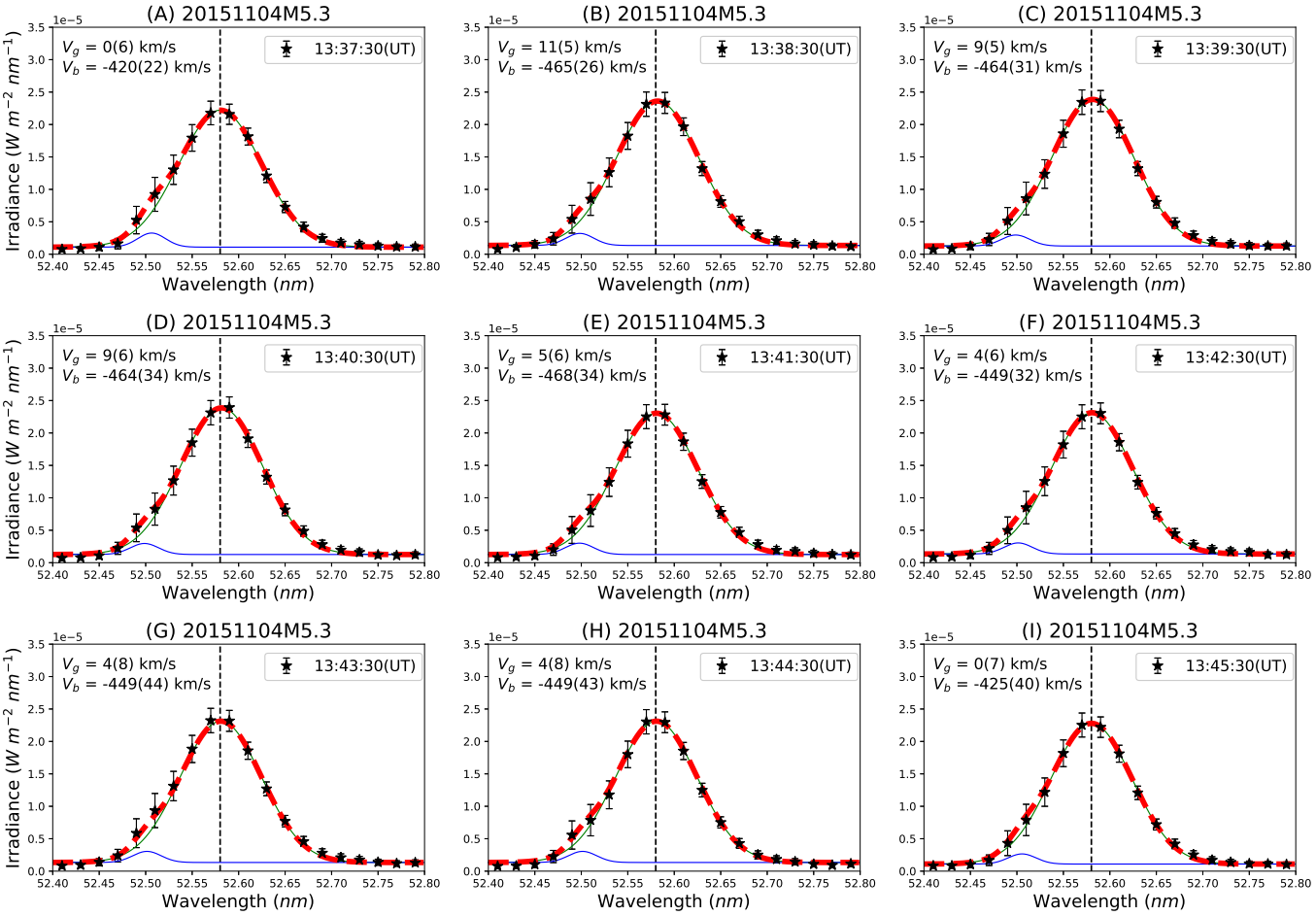

Figure 7. Double Gaussian fitting results for nine O III 52.58 nm line profiles taken during CME 5 (20151104M5.3). The nine panels are similar to those in Figure 3 of the paper.

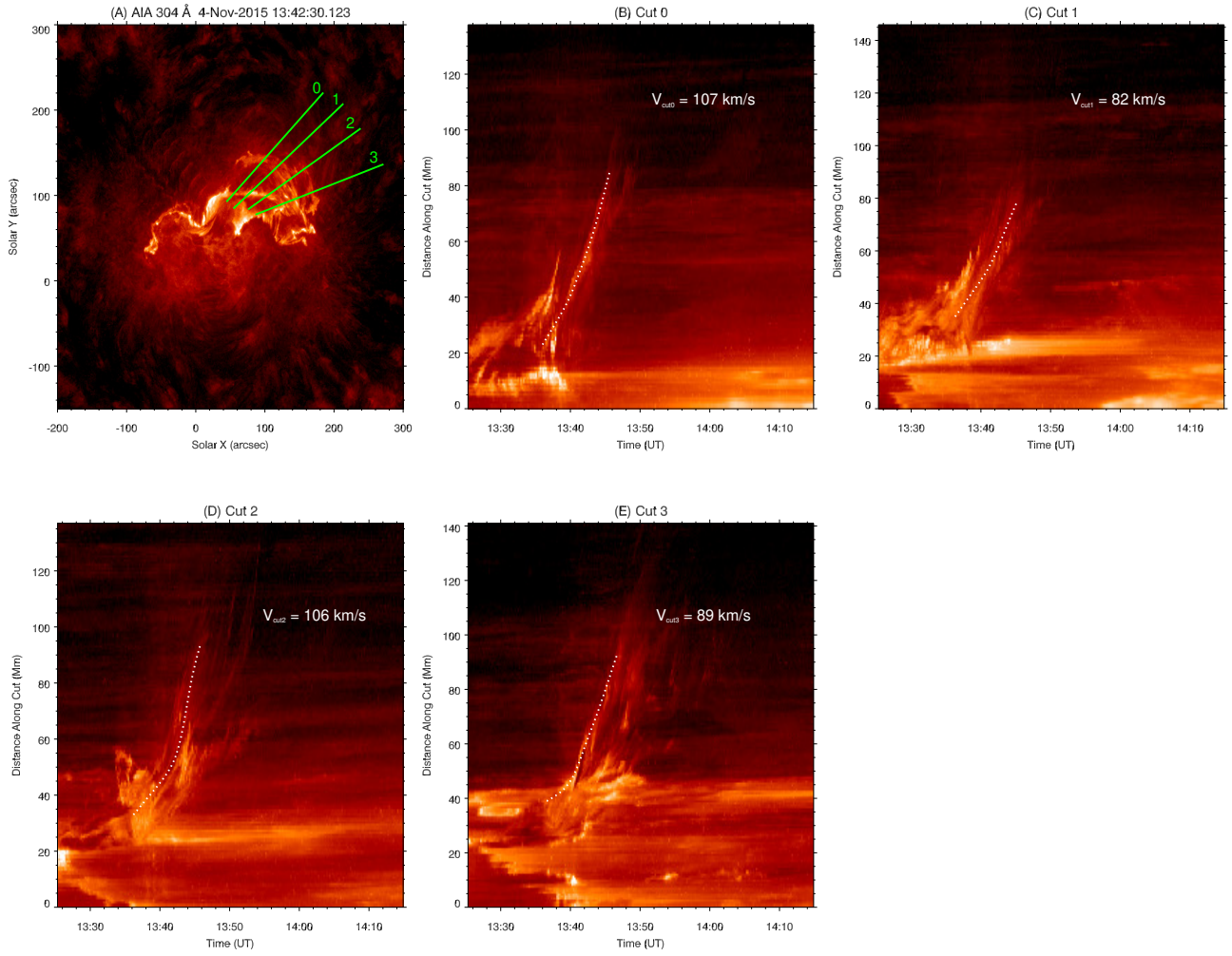

Figure 8. Ejecta associated with CME 5 (20151104M5.3) in SDO/AIA 30.4 nm images. The five panels are similar to those in Figure 4 of the paper.
(An animation of this figure is available.)

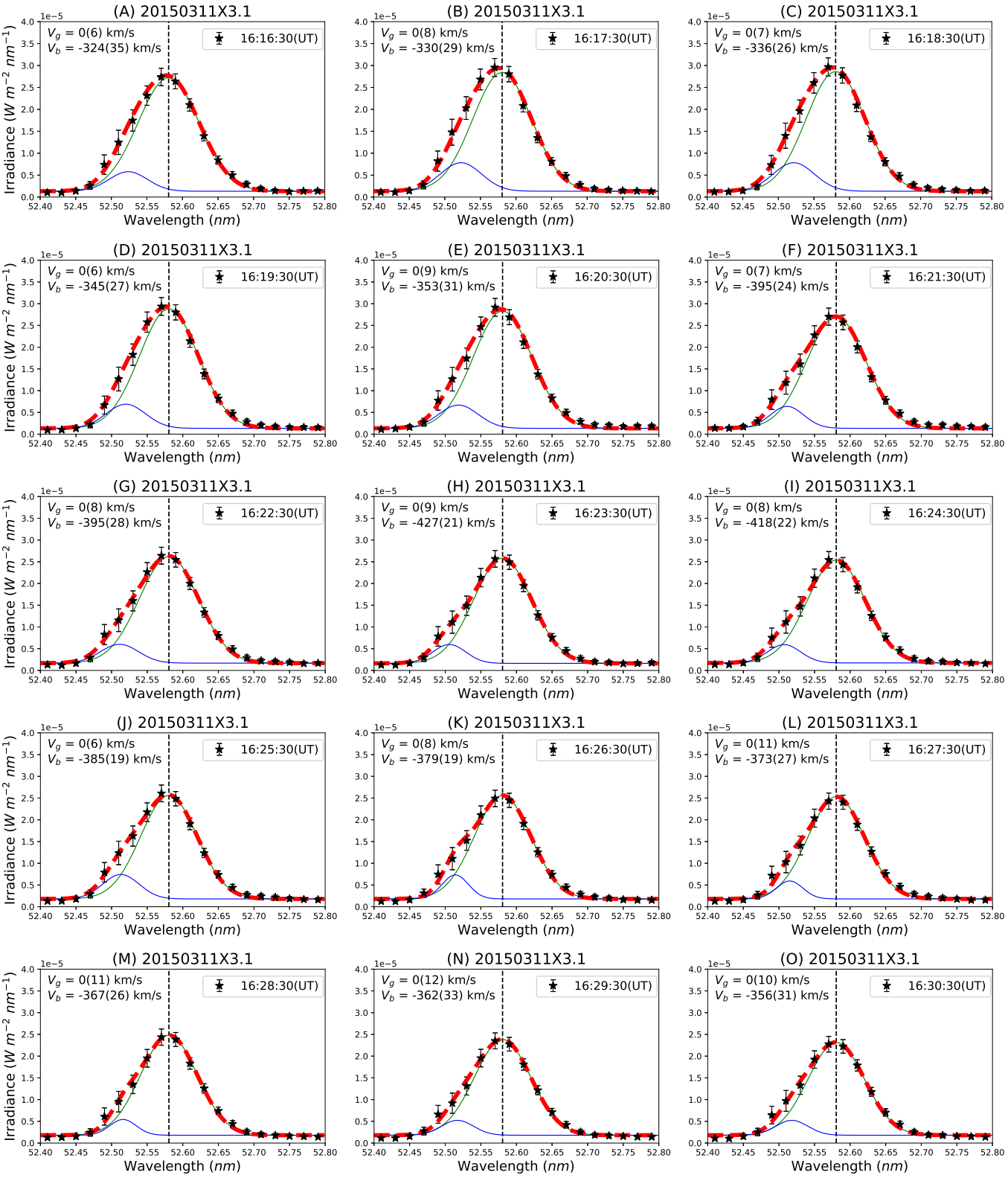

Figure 9. Double Gaussian fitting results for fifteen O III 52.58 nm line profiles taken during CME 6 (20150311X3.1). The fifteen panels are similar to those in Figure 3 of the paper.

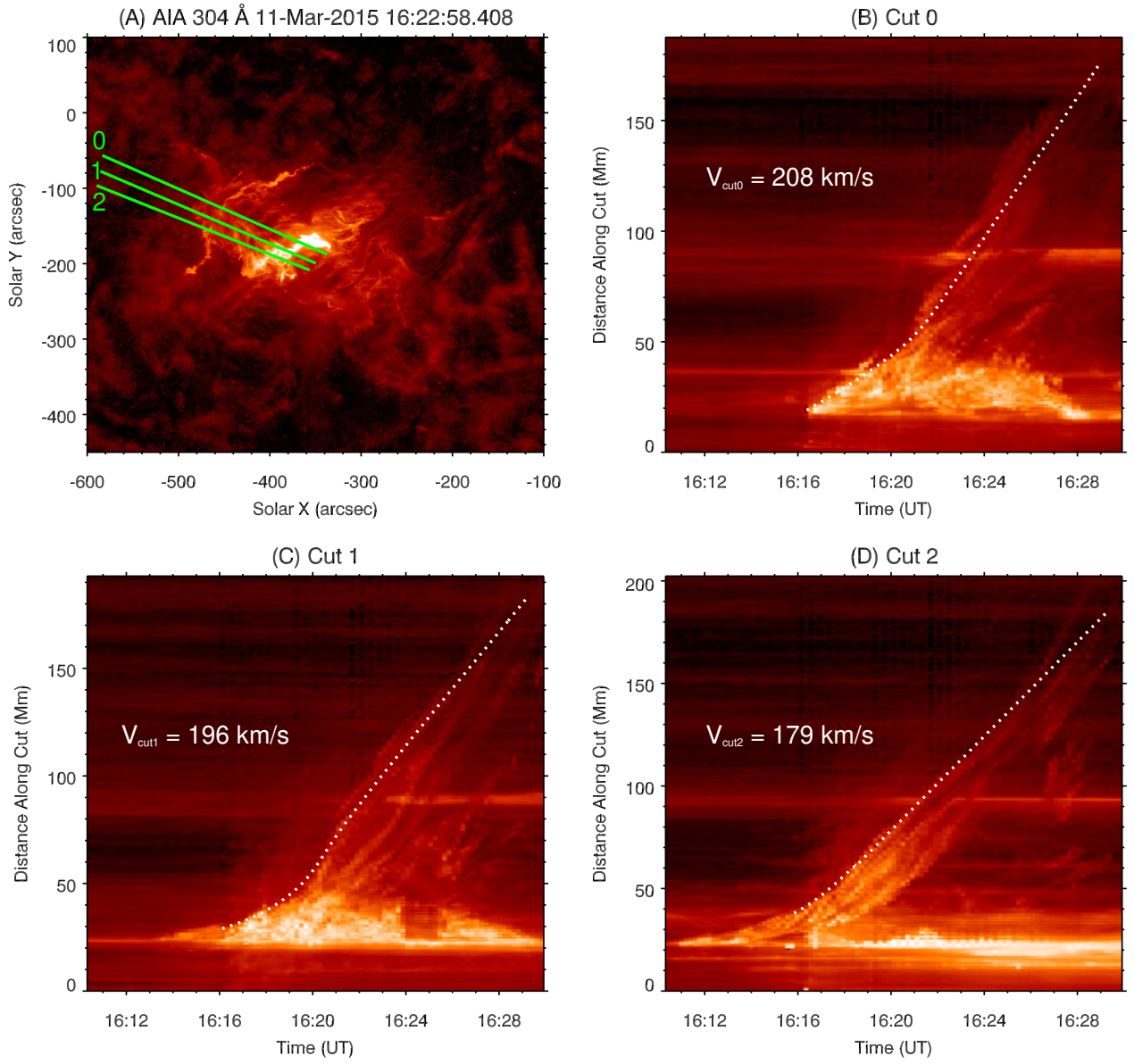

Figure 10. Ejecta associated with CME 6 (20150311X3.1) in SDO/AIA 30.4 nm images. The four panels are similar to those in Figure 4 of the paper.
(An animation of this figure is available.)

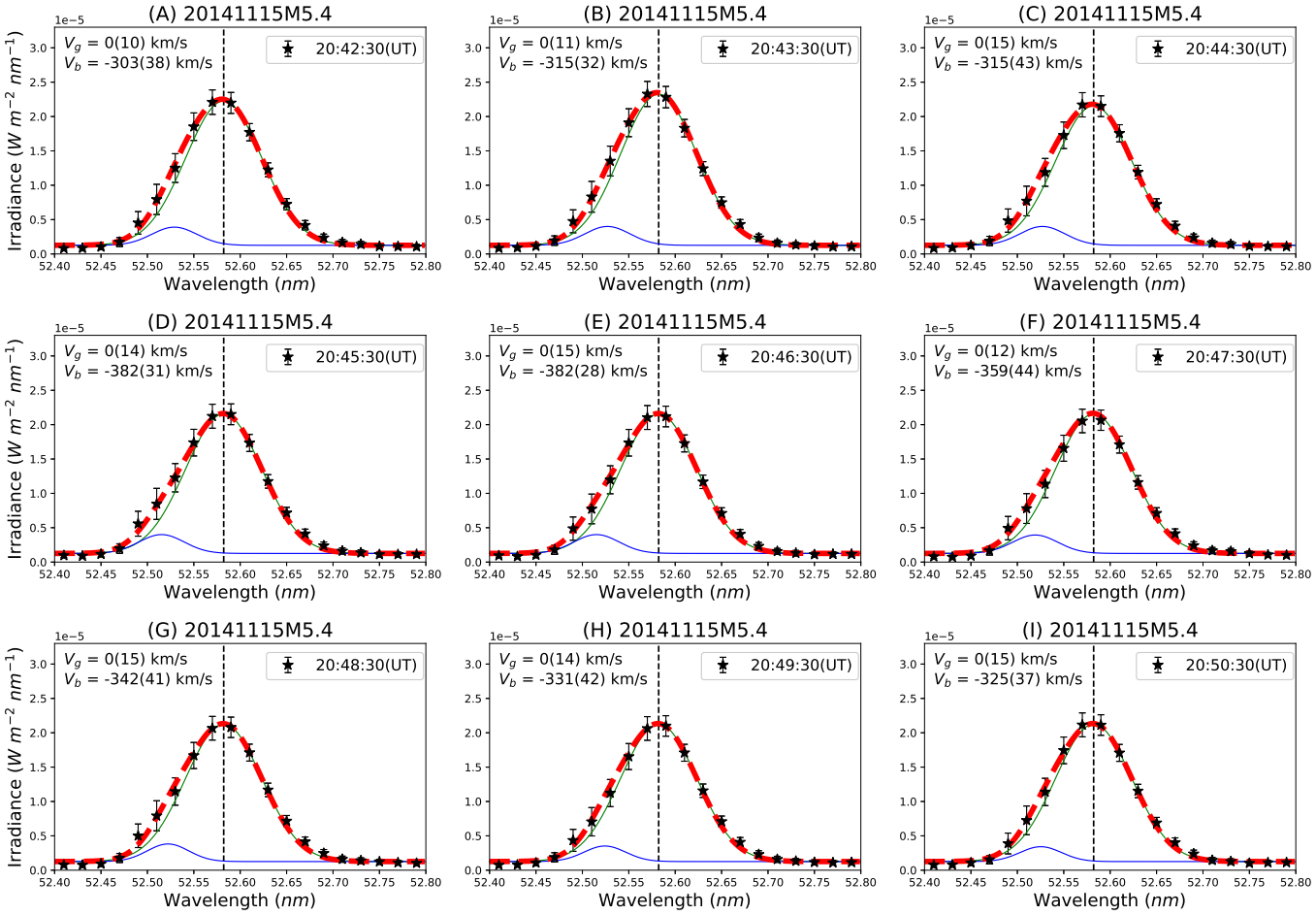

Figure 11. Double Gaussian fitting results for nine O III 52.58 nm line profiles taken during CME 7 (20141115M5.4). The nine panels are similar to those in Figure 3 of the paper.

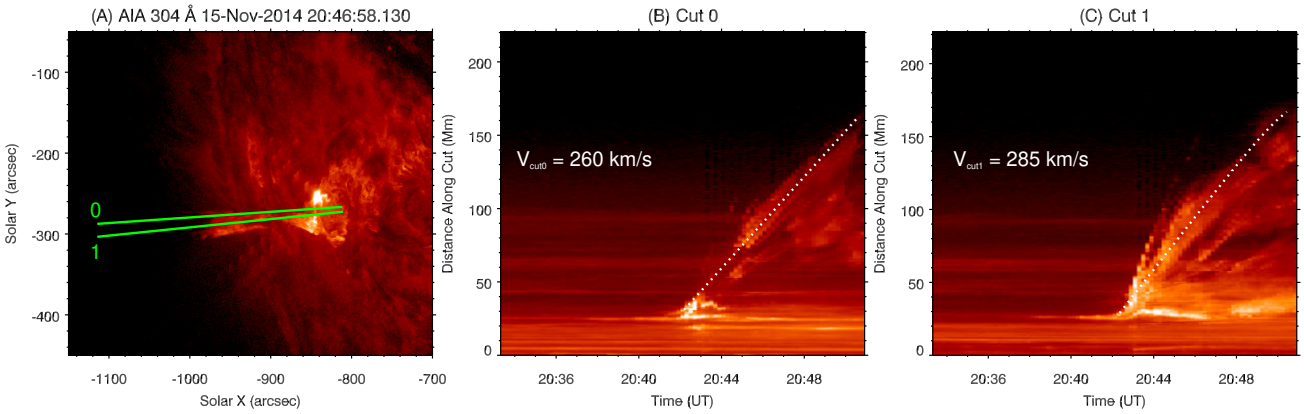

Figure 12. Ejecta associated with CME 7 (20141115M5.4) in SDO/AIA 30.4 nm images. The three panels are similar to those in Figure 4 of the paper.
(An animation of this figure is available.)

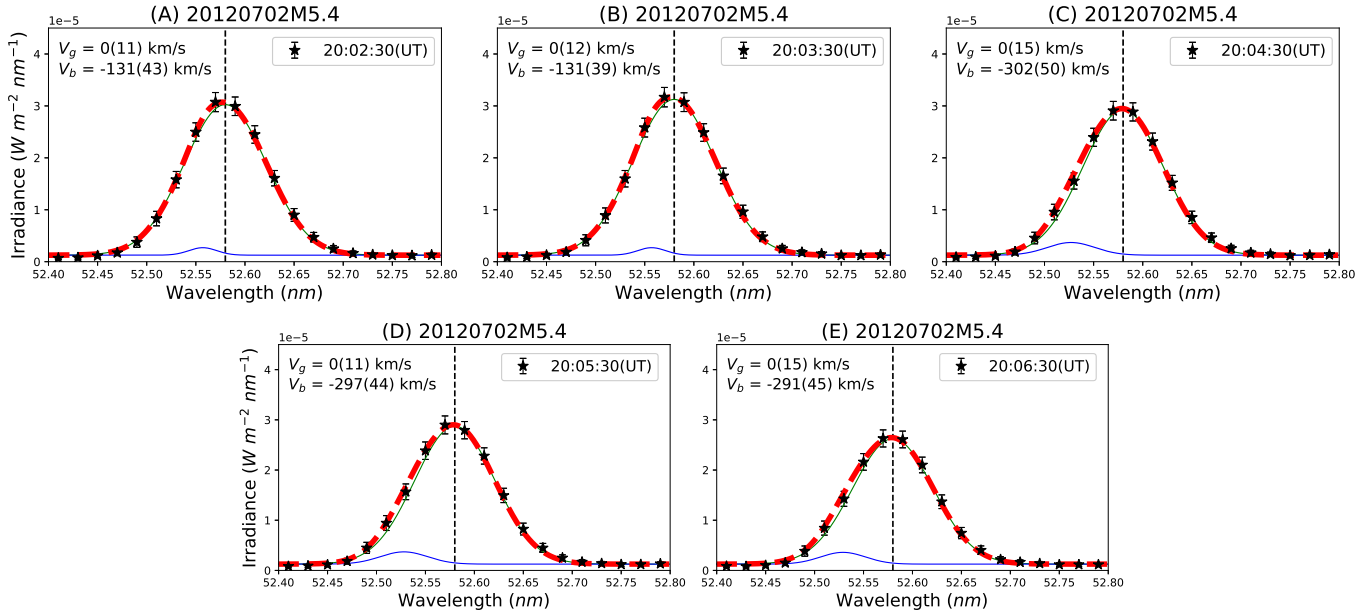

Figure 13. Double Gaussian fitting results for five O III 52.58 nm line profiles taken during CME 8 (20120702M5.4). The five panels are similar to those in Figure 3 of the paper.

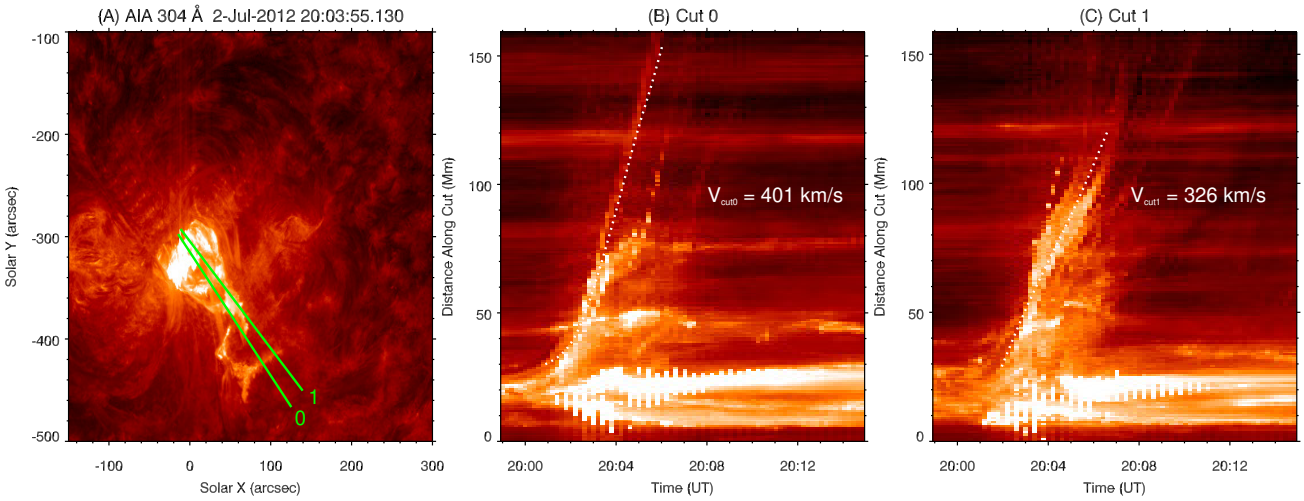

Figure 14. Ejecta associated with CME 8 (20120702M5.4) in SDO/AIA 30.4 nm images. The three panels are similar to those in Figure 4 of the paper.
(An animation of this figure is available.)